

AD-A265 240



(2)

OFFICE OF NAVAL RESEARCH

GRANT N00014-89-J-1178

R&T CODE 413Q001-05

TECHNICAL REPORT NO. #59

**IN-SITU INVESTIGATION OF TEMPERATURE AND BIAS DEPENDENT
EFFECTS ON THE OXIDE GROWTH OF Si AND Ge IN AN ECR PLASMA**

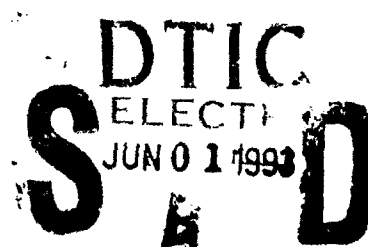
Y.Z. Hu, Y.Q. Wang, M. Li, J. Joseph, and E.A. Irene
Department of Chemistry
University of North Carolina at Chapel Hill
Chapel Hill, NC 27599-3290

Submitted to:

Journal of Vacuum Science and Technology

**Reproduction in whole or in part is permitted for any purpose of the United States
Government.**

**This document has been approved for public release and sale; its distribution is
unlimited.**



93 01 3

93-12130



KIP

REPORT DOCUMENTATION PAGE

Form Approved

OMB No. 0704-0188

Public reporting burden for this collection of information is estimated to average 1 hour per response, including the time for reviewing instructions, searching existing data sources, gathering and maintaining the data needed, and completing and reviewing the collection of information. Send comments regarding this burden estimate or any other aspect of this collection of information, including suggestions for reducing this burden, to Washington Headquarters Services, Directorate for Information Operations and Reports, 1215 Jefferson Davis Highway, Suite 1204, Arlington, VA 22202-4302, and to the Office of Management and Budget, Paperwork Reduction Project (0704-0188), Washington, DC 20503.

1. AGENCY USE ONLY (Leave blank)

2. REPORT DATE

5/4/93

3. REPORT TYPE AND DATES COVERED

4. TITLE AND SUBTITLE

In-Situ Investigation of Temperature and Bias Dependent Effects on the Oxide Growth of Si and Ge in an ECR Plasma.

5. FUNDING NUMBERS

#N00014-89-J-1178

6. AUTHOR(S)

Y.Z. Hu, Y.Q. Wang, M. Li, J. Joseph, and E.A. Irene

7. PERFORMING ORGANIZATION NAME(S) AND ADDRESS(ES)

The University of North Carolina
Chemistry Department
CB #3290 Venable Hall
Chapel Hill, NC 27599-3290

8. PERFORMING ORGANIZATION REPORT NUMBER

Technical Report#59

9. SPONSORING / MONITORING AGENCY NAME(S) AND ADDRESS(ES)

Office of Naval Research
800 N. Quincy Street
Arlington, VA 22217-5000

10. SPONSORING / MONITORING AGENCY REPORT NUMBER

11. SUPPLEMENTARY NOTES

None

12a. DISTRIBUTION / AVAILABILITY STATEMENT

This document has been approved for public release and sale, distribution of this document is unlimited.

12b. DISTRIBUTION CODE

13. ABSTRACT (Maximum 200 words)

The electron cyclotron resonance, ECR, plasma oxidation of Si and Ge was investigated using in-situ spectroscopic ellipsometry at substrate temperatures of 80 to 400 °C and at bias voltages of -30 to +60 V. A study of the oxide growth kinetics by ECR plasma oxidation results in three distinct regions of growth with the first two being linear and the last parabolic. At the earliest linear stage the rate of oxide growth is the fastest, and corresponds to around 3 nm film thickness which is not dependent on bias. Following this, the second linear region displays an oxide growth rate proportional to the bias with typical growth rates of 0.10, 0.32 and 0.60 nm/min for 0, +30 and +60V, respectively, at 300 °C. The third region displays parabolic kinetics and corresponds to the Cabrera-Mott, C-M, theory for the oxidation by charged species in the limit of a low electric field. Activation energies of 0.19 and 0.28 eV are obtained using the C-M model for the ECR plasma oxidation of Si and Ge, respectively.

14. SUBJECT TERMS

Oxide growth, Plasma

15. NUMBER OF PAGES

16. PRICE CODE

17. SECURITY CLASSIFICATION OF REPORT

Unclassified

18. SECURITY CLASSIFICATION OF THIS PAGE

Unclassified

19. SECURITY CLASSIFICATION OF ABSTRACT

Unclassified

20. LIMITATION OF ABSTRACT

IN-SITU INVESTIGATION OF TEMPERATURE AND BIAS DEPENDENT EFFECTS ON THE OXIDE GROWTH OF Si AND Ge IN AN ECR PLASMA

Y.Z. Hu, Y.Q. Wang, M. Li, J. Joseph and E.A. Irene

Department of Chemistry, CB# 3290

University of North Carolina

Chapel Hill, NC 27599-3290

ABSTRACT

The electron cyclotron resonance, ECR, plasma oxidation of Si and Ge was investigated using in-situ spectroscopic ellipsometry at substrate temperatures of 80 to 400 °C and at bias voltages of -30 to +60 V. A study of the oxide growth kinetics by ECR plasma oxidation results in three distinct regions of growth with the first two being linear and the last parabolic. At the earliest linear stage the rate of oxide growth is the fastest, and corresponds to around 3 nm film thickness which is not dependent on bias. Following this, the second linear region displays an oxide growth rate proportional to the bias with typical growth rates of 0.10, 0.32 and 0.60 nm/min for 0, +30 and +60 V, respectively, at 300°C. The third region displays parabolic kinetics and corresponds to the Cabrera-Mott, C-M, theory for the oxidation by charged species in the limit of a low electric field. Activation energies of 0.19 and 0.28 eV are obtained using the C-M model for the ECR plasma oxidation of Si and Ge, respectively. Increasing the negative bias causes oxide sputter etching and surface damage, with no significant contribution to oxidation. A probable mechanism for the ECR plasma oxidation process is also discussed.

For	
1	<input checked="" type="checkbox"/>
2	<input type="checkbox"/>
3	<input type="checkbox"/>
4	

By	
Distribution/	
Availability Codes	
Dist	Avail and/or Special
A-1	

I. INTRODUCTION

Low temperature processing of semiconductors is of interest since rates for thermally activated defect production and redistribution of impurities are greatly reduced. Plasma oxidation, utilizing an oxygen plasma is a promising low temperature technique used to grow dielectric films on semiconductor surfaces. Microwave electron cyclotron resonance, ECR, plasmas have much higher fractional ionization (up to 10%), longer ion and energetic neutral mean free paths, and lower maximum ion energies than conventional rf parallel-plate discharges¹. Recently an ECR oxygen plasma has been used to grow silicon dioxide from single crystal silicon²⁻⁵, exhibiting the physical, chemical and electrical properties similar to those of high temperature thermally grown oxides. However, reports on the ECR plasma oxidation of Ge appear to be lacking. Although the ECR plasma oxidation of semiconductor materials are of great interest, the kinetics and mechanisms involved are complicated and thus are not yet fully understood.

The work presented in this paper focuses on a kinetic study of the various parameters influencing the oxidation process of Si and Ge, using both in-situ static spectroscopic ellipsometry, SE, and dynamic real time single wavelength ellipsometry, SWE. The dependence of oxide growth on time, substrate temperature and bias voltage are presented along with a growth model based on that of Cabrera and Mott^{5,6}.

II. EXPERIMENTAL TECHNIQUE

The ECR plasma oxidation equipment used in this study was described previously⁵. A 2.45 GHz microwave, as generated by a magnetron, is guided through a quartz window to the ECR

plasma source chamber filled with oxygen gas (99.997%) that was taken directly from a cylinder without further purification. The vacuum chamber can be evacuated to 5×10^{-8} Torr using a turbomolecular pump. The substrate to be oxidized is placed on a stainless steel holder that can be heated using a halogen lamp. The temperature was monitored and controlled using a thermocouple attached to the front side of the sample holder and adjacent to the sample. A calibration of the holder temperature was made in comparison with substrate temperature. The oxygen plasma irradiates the substrate at near normal incidence.

The plasma oxidation conditions were as follows: total pressure of 1×10^{-3} Torr, oxygen flow rate of 20 sccm, microwave power of 300 W, substrate temperature from 25°C to 400°C, and substrate bias voltages from -60 V to +60 V. The samples used were commercially available lightly doped P-type $\langle 100 \rangle$ Ge wafers and P-type $\langle 100 \rangle$ Si wafers.

The thicknesses of the oxide layers was determined by means of real time single wavelength ellipsometry. The various thicknesses reported in this work were obtained by a trajectory method^{5,7}. The single wavelengths chosen for Si and Ge are 340 and 335 nm, since the measurements are insensitive to temperature and highly sensitive to oxide growth at these wavelengths. The SE measurements were taken at 41 photon energies between 2.5 and 4.5 eV. For the measurement of each sample the offsets of analyzer and polarizer were redetermined. This was necessary to maintain the highest accuracy, because a small misalignment of the sample stage occurred with sample changes. Each spectroscopic measurement takes about 10 min and during the measurement the plasma was stopped. For the oxides grown above room temperature the spectra were obtained at room temperature after cooling the sample. This was done because of the unavailability of reliable optical data for all the components present for the higher

temperatures.

III. RESULTS AND DISCUSSION

A. Optical Modeling

Spectroscopic ellipsometry has been used extensively to study thin films grown on semiconductor materials⁸⁻¹². The ellipsometric measurement yields two angles: Δ and Ψ , from which the complex reflection ratio ρ_{exp} is obtained: $\rho_{exp} = \tan \Psi e^{i\Delta}$. From a literature database for the known constituents of the film and substrate, ρ_{cal} is calculated and compared with ρ_{exp} and as figure of merit for comparison, an unbiased estimator δ is calculated from the relationship^{5,13}:

$$\delta = \left[\frac{1}{N-P-1} \sum_{i=1}^N |\rho_{exp} - \rho_{cal}|^2 \right]^{1/2} \quad (1)$$

here N is the number of wavelengths sampled, and P the number of unknown parameters. A minimizing procedure gives the best fit parameters which are film thicknesses and volume percents for the constituents at the 90% confidence level.

Figure 1 shows a typical variation of the pseudo-dielectric function, $\langle \epsilon \rangle$, as obtained from SE, in terms of both ϵ_1 and ϵ_2 versus photon energy, for the plasma oxidation of Si and Ge. Four sensible models shown in Fig.2 were evaluated, and model D made up of pure oxide as the topmost layer and an interface layer composed of oxide and amorphous Si or Ge, yields the best fit in terms of the lowest δ . The calculation results from model D for both Si and Ge are also shown in Fig.1. It is interesting to observe that the best fit model for both Si and Ge ECR oxidation is the same.

B. Time Dependence of the Oxide Growth

In order to investigate the ECR plasma oxidation kinetics, the plasma oxidation of Si and Ge was performed for various times at different bias voltages and temperatures under the same plasma conditions. Figure 3 shows the typical results for the oxide thicknesses as a function of time at a microwave power of 300 W, substrate temperature of 300 °C, and three different substrate bias voltages of 0, +30 and +60 V. The results of Fig.3a and 3c show the evolution of the thickness as a function of the oxidation time, obtained by the trajectory method and a one film model from the real time single wavelength ellipsometric measurements during the first 20 and 30 min for Si and Ge, respectively. The thickness results of Fig.3b and 3d were obtained by SE using a two film model. The total thickness is given by the solid line and the interface thickness by the filled symbols. The experimental results in Fig.3 show that there are three regimes for the relationship between time and thickness. The earliest two regimes are nearly linear with the first being both the fastest and virtually bias independent. Following these linear regimes, a parabolic shape in the growth data is observed.

In order to discuss the time dependence of the oxide growth, several oxidation models, including the linear-parabolic model for Si thermal oxidation developed by Deal and Grove¹⁴ (D-G), a time power law oxidation model by Wolters and Zegers-van Duynhoven¹⁵ (W-Z) and the parabolic model by Cabrera-Mott^{6,16} (C-M), have been used^{2,5,17,18}. However, we were not successful with any of above models for the entire experimental thickness-time range of our plasma oxidation data.

Figure 4 shows a schematic of the DC potential profiles in the growing oxide as a function of the thickness³. Initially, the surface potential V_s will be equal to the bias potential V_b , i.e.,

for bare wafers or for oxides that are too thin to sustain an electric field. After the oxide has reached a thickness L_{ox} the overall oxide potential drop $V_{ox} = V_b - V_s$ will increase with increasing film thickness. Therefore, the field in the oxide will be: $E_{ox} = V_{ox}/L_{ox}$. Previous experimental results also indicated that negatively charged oxygen atoms formed at the plasma-oxide interface are the primary oxidant under anodic oxidation conditions^{2,3,5,12,17}. The field E_{ox} may lead to rapid transport of ionic species through the oxide.

Since the oxidizing species react at the plasma-wafer interface without transport in the first linear regime where $E_{ox}=0$, the oxidation is bias independent. In the second linear regime the electric field develops in the thin oxide layer, and the oxidizing ionic species transports rapidly by the field due to low transport resistance. Thus the film growth remains reaction limited, but it now is electric field dependent. These two linear regimes in the early ECR plasma oxidation of Si and Ge are very similar to those formed in the early stage of Si thermal oxidation^{19,20}. From the theory by Murali and Murarka²⁰ (M-M) at the earliest stage, the oxidizing species diffuse through a very thin oxide layer into the substrate due to the low diffusion resistance of the thin oxide layer. The oxidation takes place over a reaction volume zone rather than only at the interface, and the rate of oxide growth is fast. When the oxide thickens, the oxidizing species is consumed at the interface due to an increased diffusion resistance of a thicker oxide layer. According to M-M model there is a critical thickness, L_{ox}^* , below which the oxide growth is given by a high growth rate. For the thicknesses greater than L_{ox}^* the growth is given by a second slower rate. The critical thickness is not bias dependent, but it is dependent on the substrate temperature. From Fig.3a and 3c and our previous paper⁵ typical values of L_{ox}^* are about 1.5 nm (for Si) at room temperature and about 3 nm (for Si and Ge) at 300 °C. Following

these linear regimes, parabolic growth is observed which agrees with the C-M model^{5,6,16} which includes electric field effects resulting from the applied biases.

C. Bias Dependence of the Oxide Growth

The reactive species generated in oxygen plasmas are positive ions, negative ions, electrons and neutrals. Positive or negative bias applied on the substrate causes different effects, since the effected reactive species is different. For a constant positive applied bias voltage, the dominant reactive species are likely to be O^+ and O .

According to the C-M model for oxidation by charged species in the limit of a low electric field, the growth rate is given by the relationship:

$$L_{ox}^2 = C_1 \exp\left[-\frac{E_a}{KT}\right] \frac{V_{ox}}{KT} t + C_2 \quad (2)$$

where V_{ox} is the potential drop across the oxide film, E_a is the thermal activation energy associated with the diffusivity of oxidizing species in the applied electric field, t the time, K the Boltzman constant, T the absolute temperature, and C_1 and C_2 are constants. In order to compare our experimental results to C-M model, the dependence of the parabolic coefficient, B , with the bias, shown in Fig.5b and 5d, is examined and is given as:

$$B = \frac{d(L_{ox}^2)}{dt} = k_b V_b + C_b \quad (3)$$

where V_b is bias voltage, C_b and k_b are constants. Figure 6 shows the parabolic coefficient dependence to be approximately linear with bias and using the values of $k_b=0.25 \text{ nm}^2/\text{min}\cdot\text{V}$ for Ge and $k_b=0.023 \text{ nm}^2/\text{min}\cdot\text{V}$ for Si. It is clear from eq.(2) and eq.(3) that the relationship between V_{ox} and the bias, V_b , is approximately linear. The increase of the growth rate with the

positive bias (on the Ge and Si) indicates that the negative oxygen ions are the principal oxidant species. These ions may come from the plasma itself or be formed at the surface via electron attachment to the neutral O_2 and O . The attachment is a favored process and causes decomposition of O_2 . Evidence for this has been observed for thermal oxidation²¹ and electron stimulated oxidation of Si^{22,23}. At negative bias positive oxygen ions and atoms are the likely dominant reactive species. An increase of the negative bias results in oxide sputter etching and surface damage.

D. Temperature Dependence of the Oxide Growth

The temperature dependence of the oxide film growth is determined from the data in Fig. 5a and 5c at oxidation temperatures from room temperature to 400°C. The C-M model predicts that the parabolic coefficient follows an Arrhenius expression, and this is confirmed for our results in Fig. 7a. The linear fit of these data yields an apparent activation energy, E_a . The values are 0.28 eV and 0.19 eV for the plasma oxidation of Ge and Si, respectively. It is interesting to notice that the oxide growth rate on Si is higher than that for Ge at low temperatures for ECR plasma oxidation. It is well known that the oxide growth rate of Si is much smaller than Ge in thermal oxidation. For a comparison between plasma and thermal oxidation, we measured the Ge oxide growth rate at the oxidation temperatures from 400 to 550 °C. Figure 7b shows the parabolic coefficient dependence on temperature for the thermal oxidation of Si and Ge, with the value for Si at about one order of magnitude smaller than that of Ge. This clearly indicates a very different oxidation mechanism for the ECR and thermal processes. The ECR plasma environment contains atomic charged oxidant species, and as indicated above in the bias effect measurements the negative oxidant species, likely O^- are causative. In the fields existing in the

ECR system under bias and no bias conditions these charged species are affected by the electric field. Thus, the transport of the smaller O^- species, as compared with molecular O_2 for thermal oxidation, in both a concentration and field gradient is probably the reason for the large difference in the activation energies.

IV. CONCLUSIONS

A comparison of the ECR plasma oxidation between Ge and Si shows that the ECR plasma oxidation is very similar to thermal oxidation in some points and greatly different for other points.

The similarities are:

1. The oxide structure is two layer: a pure oxide on top and an interface layer.
2. The kinetics of oxide growth shows three oxidation regimes: two linear and one parabolic.
3. The oxide properties are similar.

The differences are:

1. The dominant oxidizing species is negative oxygen ions for plasma, but molecules for thermal oxidation.
2. The oxidation rate is bias dependent.
3. The activation energies in the plasma oxidation of Si and Ge are much smaller than those in thermal oxidation.
4. In low temperature ECR plasma oxidation, the oxide growth rate of Si is higher than that for Ge which is reversed for thermal oxidation.

ACKNOWLEDGMENTS

This work was supported in part by the National Science Foundation, NSF, and the Office of Naval Research, ONR.

REFERENCES

1. T. Ono, C. Takahashi, and S. Matsuo, Jpn. J. Appl. Phys. 23, L534 (1984).
2. D.A. Carl, D.W. Hess, M.A. Lieberman, J. Vac. Sci. Technol. A 8 2924, (1990).
3. D.A. Carl, D.W. Hess, M.A. Lieberman, T.S. Nguyen and R. Gronsky, J. Appl. Phys., 70, 3301 (1991).
4. G.T. Salbert, D.K. Reinhard, and J. Asmussen, J. Vac. Sci. Technol. A 8, 2919 (1990).
5. J. Joseph, Y.Z. Hu and Irene, J. Vac. Sci. Technol. B 10, 611 (1992).
6. N. Cabrera and N.F. Mott, Rep. Prog. Phys. 12, 163 (1948).
7. A. Gagnaire, J. Joseph, and A. Etcheberry, J. Electrochem. Soc. 134, 2476 (1987).
8. D.E. Aspnes and A.A. Studna, Phys. Rev. B, 27, 985 (1983).
9. D.E. Aspnes, W.E. Quinn and S. Gregory, Appl. Phys. Lett., 56, 2569 (1990).
10. R.W. Collins, Rev. Sci. Instrum., 61, 2069 (1990).
11. R.W. Collins, J. Vac. Sci. Technol. A, 7, 1378 (1989).
12. Y.Z. Hu, J. Joseph and E.A. Irene, Appl. Phys. Lett., 59, 1353 (1991).
13. D.E. Aspnes, J.B. Theeten, and F. Hottier, Phys. Rev. B, 20, 3992 (1979).
14. B.E. Deal and A.S. Grove, J. Appl. Phys., 36, 3770 (1965).
15. D.R. Wolters and A.T.A. Zegers-van Duynhoven, J. Appl. Phys., 65, 5134 (1989).
16. F.P. Fehlner, J. Electrochem. Soc., 131, 1645 (1984).

17. S. Kimura, E. Murakami, K. Miyake, T. Warabisako, H. Sunami, and T. Tokuyama, J. Electrochem. Soc., 132, 1460 (1985).
18. C. Vinckier, P. Coeckelberghs, G. Stevens, M. Heyns, and S. De Jaegere, J. Appl. Phys., 62, 1450 (1987).
19. E.A. Irene, J. Electrochem. Soc., 125, 1708 (1978).
20. V. Murali and S.P. Murarka, J. Appl. Phys., 60, 1206 (1986).
21. E.A. Irene and E.A. Lewis, Appl. Phys. Lett., 51, 767 (1987).
22. P. Collot, G. Gautherin, B. Agius, S. Rigo and F. Rochet, Phil. Mag. B, 52, 1051 (1985).
23. A. Miotello and F. Toigo, Phil. Mag. Lett., 55, 53 (1987).

FIGURE CAPTIONS

Figure 1. Pseudo-dielectric function of Si (a) and Ge (b). Experimental data after ECR plasma oxidation are presented by symbols. The solid lines are before oxidation. The dashed lines correspond to an two layer model (model D in Fig.2) calculation.

Figure 2. Four optical models used to evaluate the SE data of Fig.1. The top is for Si oxidation and the bottom is for Ge oxidation.

Figure 3. Thicknesses of the grown oxide layer vs ECR plasma oxidation time for three biases. (a) and (b) are for Si oxidation at room temperature; (c) and (d) are for Ge oxidation at 300 °C; (a) and (c) Thicknesses are calculated at single wavelength using a one layer model; (b) and (d) Thicknesses are calculated from SE data using model D in Fig.2. The solid lines are for total thicknesses. The interface layer thicknesses are represented by filled symbols.

Figure 4. Schematic diagram of potential profiles in the growing oxide at constant positive bias voltage: (a) Initial growth; (b) thicker oxide.

Figure 5. Square of total oxide thickness vs the oxidation time from SE data for various temperatures and biases: (a) Si at +30 V; (b) Si at room temperature; (c) Ge at +20 V; (d) Ge at 300 °C.

Figure 6. Parabolic coefficients deduced from linear fit of the data in Fig.5(b) and (d) vs applied bias: (a) Si; (b) Ge.

Figure 7. Arrhenius plots of the parabolic coefficients: (a) plasma oxidation of Si and Ge, data deduced from Fig.5 (a) and (c); (b) thermal oxidation of Si and Ge. The data for Si are from Ref.14.

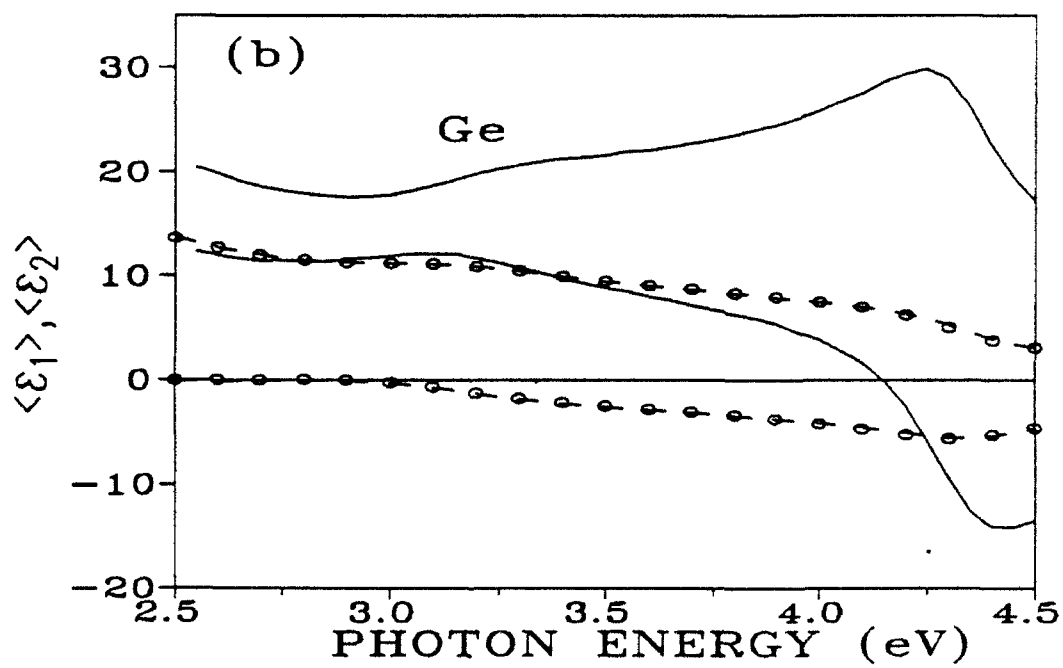
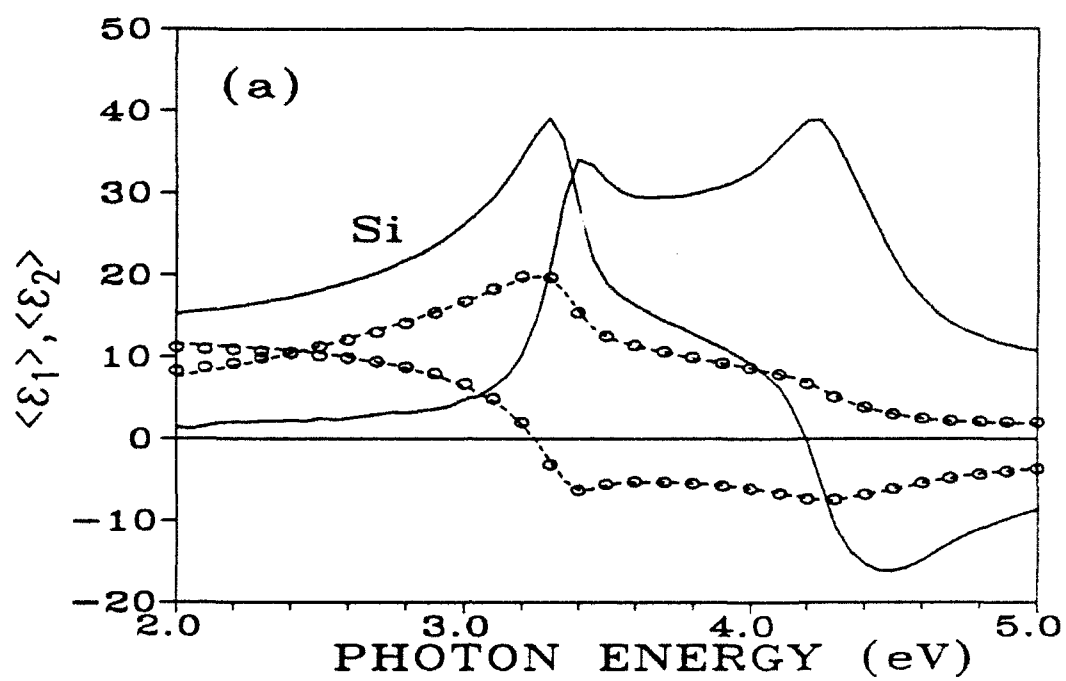


Fig 1

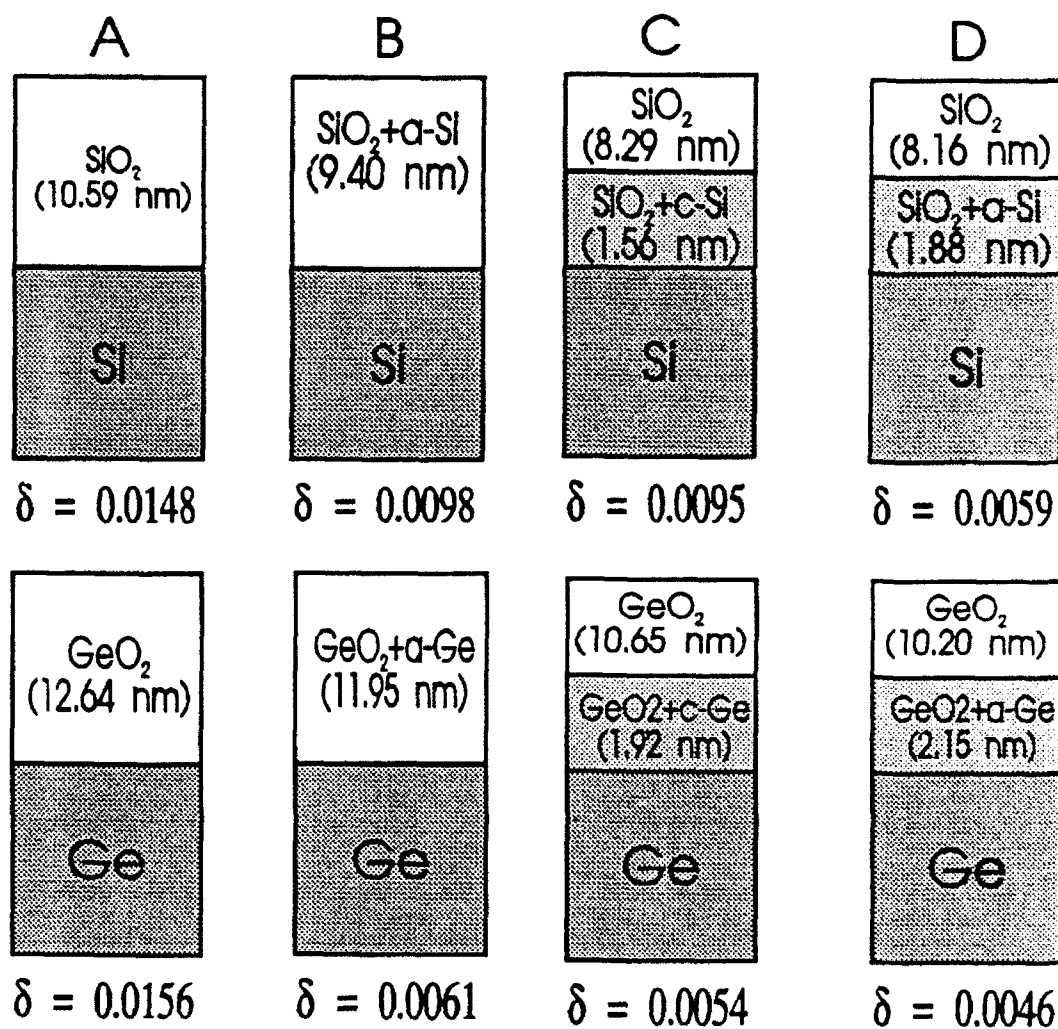


Fig. 2

